

## Crystallization, microstructure and expansivity of spodumene-orthoclase glasses

Esmat M. A. Hamzawy

Glass Research Department, National Research Centre, Cairo (Egypt)

---

The crystallization behaviour was investigated for some glasses, within the system spodumene-orthoclase, during different heat treatments by DTA, XRD and SEM. Kaolin and quartz sand were used as starting materials for the glass preparation and melting. The base glasses were stable through the heat treatments and did not show any crystallization propensity, whereas TiO<sub>2</sub> additions catalyze the crystallization tendency in the glasses. The crystallization process involved the formation of  $\beta$ -spodumene and leucite in addition to the metastable high quartz, which disappeared at higher temperatures (>900 °C). Translucent glass-ceramics, containing uniform and nonuniform microstructures, were obtained in the case of domination of high quartz and  $\beta$ -spodumene, respectively.

Little difference in the coefficient of thermal expansion (CTE) was noted in the base glasses ( $64$  to  $66 \cdot 10^{-7} \text{ K}^{-1}$  at  $20$  to  $500$  °C) and the TiO<sub>2</sub> doped glasses ( $60$  to  $69 \cdot 10^{-7} \text{ K}^{-1}$  at  $20$  to  $500$  °C). Change in CTE in the TiO<sub>2</sub> doped glass-ceramic samples from  $37$  to  $69 \cdot 10^{-7} \text{ K}^{-1}$  at  $20$  to  $300$  °C depends mainly on the content of crystallized  $\beta$ -spodumene in addition to the residual glass. However, an increase in  $\beta$ -spodumene content in the crystallized glass-ceramics lowers the value of CTE and vice versa.

---

### 1. Introduction

It is well known that the phase formation in the ternary K<sub>2</sub>O–Al<sub>2</sub>O<sub>3</sub>–SiO<sub>2</sub> system is very difficult [1]. Leucite is the known crystalline phase usually developed in glass samples of this system [2]. It is formed according to the mechanism of surface nucleation and crystallization [3]. Because the crystallization of such phase is difficult, the catalytic effect of seeding and elastic strains are of particular interest [4 and 5]. Therefore, it is highly probable that reactive surfaces of the glass powder particles initiate crystallization [6]. Consequently, they catalyze the formation of leucite in glass powders with low fluorine content [7]. Crystallization and coupled substitution of B and K for Si in leucite were detected by the sol gel method [8]. In the production of bricks, tiles, and clay pipe, leucite was obtained by thermal decomposition of natural muscovite mica [9]. In recent years, leucite based glass-ceramic has been used for dental prostheses [10 and 11].

On the other hand, the easily nucleated lithium aluminium silicate phases, i.e. spodumene and eucryptite, have very low thermal expansion and excellent thermal and chemical durability [12]. As to the latter properties, many authors improved such glass-ceramics through the crystallization of many glass systems based on lithium aluminium silicate compositions [13, 14 and 15].

The ternary system of spodumene-nepheline-orthoclase glasses is the subject of this study to show glass formation,

crystallization and thermal expansivities. The work is focused on a part of the ternary system, i.e. the binary spodumene-orthoclase subsystem with and without addition of TiO<sub>2</sub>. The effect of heat treatment on the developed phases and microstructures will be discussed. The thermal expansivity of such glasses and glass-ceramics will also be studied.

### 2. Experimental

Local kaolin and quartz sand were used as starting materials for glass batch preparations. Kaolin was obtained from the El-Tieh area (Sinai, Egypt) and has the following composition (in wt%): 44.20 SiO<sub>2</sub>, 37.75 Al<sub>2</sub>O<sub>3</sub>, 0.93 Fe<sub>2</sub>O<sub>3</sub>, 1.85 TiO<sub>2</sub>, 0.82 CaO, 0.52 MgO, 0.72 K<sub>2</sub>O and 1.15 Na<sub>2</sub>O, with 12.08 ignition loss. Other additives like lithium and potassium were introduced into the batches as carbonates and a little TiO<sub>2</sub> as nucleating agent. The batches were designed, calculated and weighed according to the ratio between spodumene (LiAlSi<sub>2</sub>O<sub>6</sub>) and orthoclase (KAlSi<sub>3</sub>O<sub>8</sub>) compositions given in table 1. The glass batches were melted and homogenized in a Pt crucible in an electric global furnace at a temperature of  $\approx 1550$  °C for 2 h. Due to the high viscosity of glass, the melt was quenched in air and bulk glass pieces were produced. These glass pieces were annealed at 450 °C and used for experimental processes. The heat treatment was scheduled in single stage at 900, 1000 and 1100 °C or double stage at 650 to 850 °C.

The DTA scans of the glasses were carried out using a Perkin-Elmer microdifferential thermoanalyzer (Perkin

---

Received 22 October 2003, revised manuscript 14 January 2004.

Table 1. Main chemical composition of the glass batches

glass code	nominal ratio*) spod/ortho	glass composition in wt%				
		SiO <sub>2</sub>	Al <sub>2</sub> O <sub>3</sub>	K <sub>2</sub> O	Li <sub>2</sub> O	TiO <sub>2</sub>
SO46	40 / 60	64.74	21.97	10.07	3.21	—
SO46T	40 / 60	64.74	21.97	10.07	3.21	3.00
SO55	50 / 50	64.72	22.72	8.40	4.02	—
SO55T	50 / 50	64.72	22.72	8.40	4.02	3.00
SO64	60 / 40	64.69	23.79	6.72	4.82	—
SO64T	60 / 40	64.69	23.79	6.72	4.82	3.00

\*) Portion is given in mol%.

Note:

spod: spodumene (LiAlSi<sub>2</sub>O<sub>6</sub>).

ortho: orthoclase (KAlSi<sub>3</sub>O<sub>8</sub>).

Elmer model DTA7 series). About 60 mg of the powdered glass sample, of grain size less than 0.60 mm (mesh no. 30) and greater than 0.3 mm (mesh no. 50), were used against Al<sub>2</sub>O<sub>3</sub> powder as a reference material. A heating rate of 10 K/min and sensitivity setting of 50.08  $\mu$ V/cm were maintained for all the DTA runs, which were performed under dynamic pure nitrogen atmosphere at a rate of 30 ml/min. The developed crystalline phases were identified using X-ray diffraction (Philips type: PW 1390). Using the scanning electron microscopy (SEM, Philips, XL30) the microstructures were investigated for freshly fractured samples (etched for 30 s in 1% HF, then rinsed with distilled water and coated with a thin film of gold).

The linear coefficient of thermal expansion (CTE),  $\alpha$ , of the glasses and glass-ceramics (dimension (0.3  $\times$  0.3  $\times$  1.6) cm<sup>3</sup>) was measured by dilatometry (Linseis dilatometer, model L76/1250) with a heating rate of 5 K/min. Transformation ( $T_g$ ) and softening temperatures ( $T_s$ ) were also measured for the glasses.

### 3. Results and discussion

Two groups of transparent glasses were obtained after melting three compositions of the binary spodumene-orthoclase system. The base glasses were white greenish while the TiO<sub>2</sub> containing glasses were light to dark amber in colour. The progress of the crystallization was marked by changes in the appearance of the glass samples. Consequently, the present base glasses did not show any change, but clearly perceptible change in the TiO<sub>2</sub> containing glasses was detected during the crystallization processes (table 2).

#### 3.1 DTA of the TiO<sub>2</sub> containing glasses

The DTA scans of TiO<sub>2</sub> containing glasses (figure 1) gave an endothermic effect in the 591 to 600 °C temperature range. Increase in lithium, or the nominal spodumene content, in such glasses gathers the detected broad exothermic peaks in the SO46T glass (at 662, 780, and 855 °C) and the SO55T glass (at 667, 747, and 855 °C) into a wide span pronounced peak in the SO64T glass (at 708 °C) containing the highest Li content. However, the smaller broader peaks of SO46T glass may indicate difficult nucleation and slow growth

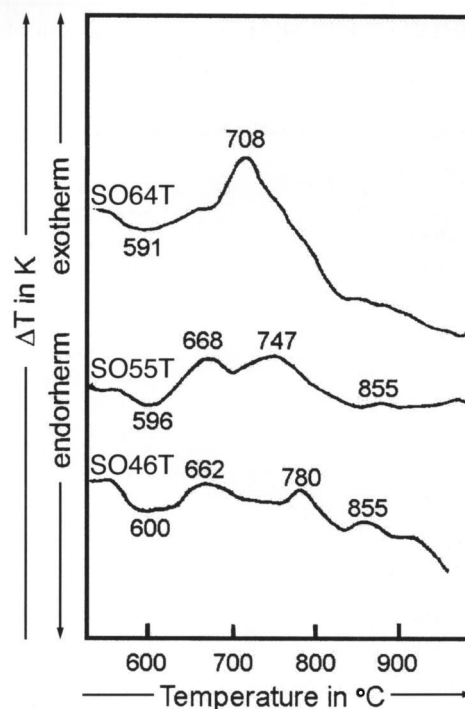


Figure 1. DTA curves of TiO<sub>2</sub> containing glasses; curve 1: SO46T glass, curve 2: SO55T glass, curve 3: SO64T glass.

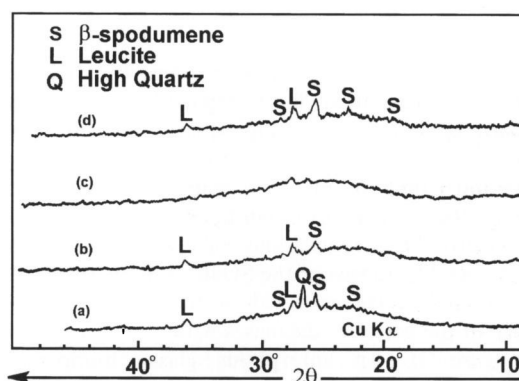


Figure 2. XRD patterns of SO46T glass heat-treated at a) 900 °C/2 h, b) 1000 °C/2 h, c) 1100 °C/2 h, and d) 650 °C/5 h and 850 °C/5 h.

whereas the pronounced clear peak of SO64T glass indicates easy and rapid crystallization.

#### 3.2 Crystallization of the glasses

The heat treatment trials on the base glasses, i.e. SO46, SO55 and SO64 samples, did not show any crystallization propensity in the single and double stage regime, however, the TiO<sub>2</sub> containing glasses, i.e. SO46T, SO55T, SO64T samples, showed varying crystallization tendency according to the glass compositions. Therefore, the X-ray diffraction analysis was used for the TiO<sub>2</sub> containing samples. Table 2 depicts the crystalline phases developed in SO46T, SO55T and SO64T glasses.

Table 2. Crystallization of TiO<sub>2</sub> containing spodumene-orthoclase glasses heat-treated at different temperatures

glass code	heat treatment parameter in °C/h	identified phase	visual morphology of the glass-ceramic sample
<b>SO46T:</b>			
–	–	amorphous	light amber glass
650/5+850/5	–	$\beta$ -spod (l)+leu (l)	yellowish creamy translucent
900/2	–	h qz+ $\beta$ -spod(l)+leu(l)	yellowish creamy translucent
1000/2	–	leu(l)+ $\beta$ -spod(l)	creamy yellowish with vitreous luster
1100/2	–	leu(t)+ $\beta$ -spod(t)	brownish glassy bands in yellowish creamy translucent
<b>SO55T:</b>			
–	–	amorphous	amber glass
650/5+850/5	–	$\beta$ -spod+leu	yellowish creamy translucent
900/2	–	$\beta$ -spod+leu+h qz(l)	yellowish creamy translucent
1000/2	–	$\beta$ -spod+leu	creamy yellowish porcelaneous
1100/2	–	$\beta$ -spod+leu	yellowish creamy translucent
<b>SO64T:</b>			
–	–	amorphous	dark amber glass
650/5+850/5	–	$\beta$ -spod+leu	yellowish creamy translucent with very fine pale violet tints in between
900/2	–	$\beta$ -spod+leu+h qz(t)	similar to above
1000/2	–	$\beta$ -spod+leu	yellowish creamy translucent
1100/2	–	$\beta$ -spod+leu	yellowish creamy translucent with very fine pale violet tints in between

Note:

leu: leucite (JCPDS no. 38-1423) [16];

$\beta$ -spod:  $\beta$ -spodumene [16]; and

h qz: high quartz (JCPDS no. 11-252) [17].

l: little, and t: trace.

Crystallization of the SO46T glass sample, with the highest potassium content, at 900 °C depicted the formation of high quartz (called quartz or high quartz as mentioned in JCPDS card no.11-252 [17]) as the main phase with  $\beta$ -spodumene and leucite (figure 2). The heat treatments of such a glass either at 1000 or 1100 °C or at 650 °C/5 h to 850 °C/5 h cleared the disappearance of high quartz. As is seen from the XRD patterns of the SO46T sample the crystallization in single stage, reflected by the intensity of d-spacing lines of the patterns, decreases with increasing temperature (figure 2). An amorphous glassy hump accompanied by a reduction in crystallization intensity was also noticed in the patterns. There is a clear indication of partial melting in the crystalline phases of the SO46T sample, at temperatures higher than 1000 °C. Visually, the yellowish creamy translucent samples were obtained at 900 °C, and at 1100 °C some fine brownish glassy bands were detected in these samples.

The XRD patterns of SO55T and SO64T glass samples heat-treated at different temperatures, i.e. at 900, 1000, 1100 and at 650 to 850 °C, showed similar phases (figure 3). It is easily predicted that the increase in Li<sub>2</sub>O/K<sub>2</sub>O ratio allows the growth of  $\beta$ -spodumene phase. Crystallization of high quartz was detected only at 900 °C in both SO55T and SO64T samples and parallel formation of  $\beta$ -spodumene and leucite phases could be observed at all the heat treatment temperatures.

Comparing the XRD patterns of leucite and  $\beta$ -spodumene phases, the higher intensity was given in the SO64T sample and the lower one in the SO46T sample. However, the optimum crystallization of both main phases was at 1000 °C.

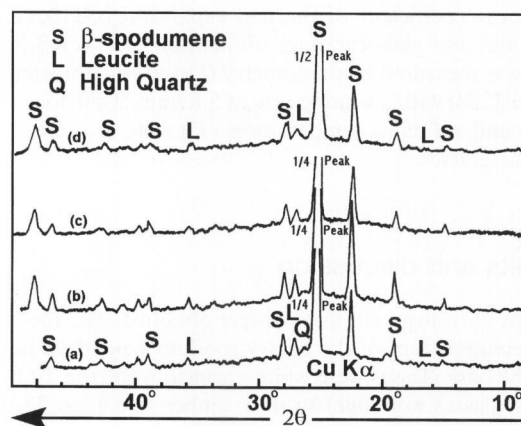


Figure 3. XRD patterns of SO64T glass heat-treated at a) 900 °C/2 h, b) 1000 °C/2 h, c) 1100 °C/2 h, and d) 650 °C/5 h and 850 °C/5 h.

Besides the disappearance of high quartz, these results indicate that the composition changes between glass SO46T and glass SO64T do not modify the crystallization and the phase transformation processes occurring in the glass but induce a strong increase in  $\beta$ -spodumene nucleation rate and in the percentage of crystalline material in the glass-ceramics.

The above mentioned results show the role of TiO<sub>2</sub> in enhancing the crystallization process in the present base glasses. In the glass-ceramic samples, crystallization of the metastable high quartz occurs at 900 °C which diminishes with increase in the Li/K ratio in the sample compositions,

or with increasing the crystallization of  $\beta$ -spodumene and leucite. However, the metastable high quartz disappears at higher temperatures ( $>900$  °C) or at double stage heat treatment. The maximum crystallization of  $\beta$ -spodumene and leucite was at 1000 °C, and the minimum crystallization was at 1100 °C, particularly in the sample containing the highest potassium content.

The increase in the tendency for crystallization reflects the magic effect of  $\text{TiO}_2$  as nucleating catalyst on the present base glasses. In the lithium aluminium silicate glasses,  $\text{TiO}_2$  acts as nucleating agent. Phase separation occurred on cooling from the melt and subsequent heating caused the formation of a number of aluminium titanate nano-crystals, which acted as sites for heterogeneous nucleation and allowed crystallization of the remaining glass to proceed [18 and 19]. Addition of  $\text{TiO}_2$  in the present spodumene-orthoclase glasses produces highly efficient nucleation, which leads to bulk crystallized glass-ceramic samples. It must be added that the presence of pale violet (tint) colour in the high lithium containing glass-ceramic sample is more properly due to the presence of various valency states of titanium. Such a tint of colour, recorded in the literature [20 and 21], may be a trace of heterogeneous immiscibility occurring during the heat treatments through the nucleation temperature.

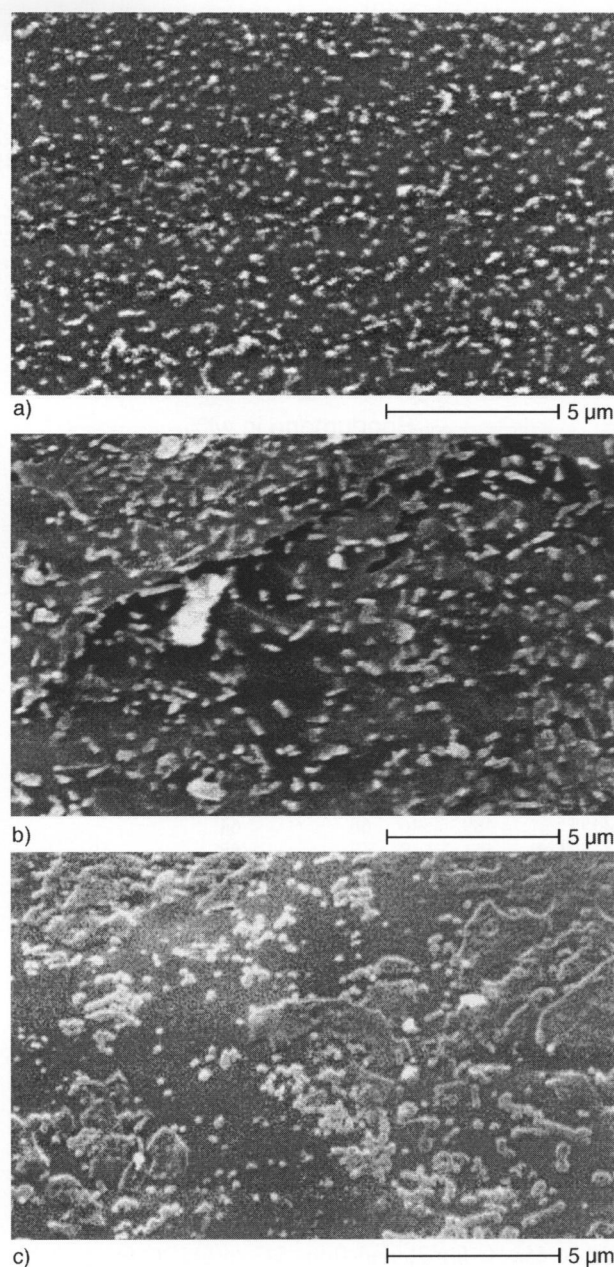
On the other hand, in the  $\text{TiO}_2$  containing glasses, the crystallization increases with the increase in the  $\text{Li}_2\text{O}/\text{K}_2\text{O}$  ratio. In contrast to  $\text{K}^{\text{rt}}$ , the  $\text{Li}^+$  enjoys higher field strength ( $\text{Li}^+ : \approx 150.69 \text{ J mol}^{-1}$ ,  $\text{K}^+ : \approx 54.42 \text{ J mol}^{-1}$  [20]) and smaller ionic radius ( $\text{Li}^+ : 0.078 \text{ nm}$ ,  $\text{K}^+ : 0.133 \text{ nm}$  [21]). This gives lithium a great tendency for easier mobility and formation of the crystalline phases.

### 3.3 Visual appearance and microstructure

The visual appearance of the crystallized samples is shown in table 2. In the present glass-ceramic samples, bulk yellowish creamy translucent materials were obtained. However, partial melting occurred at 1100 °C in the SO46T sample and brown glassy bands in yellowish creamy translucent specimens were developed.

The microstructure of SO46T, SO55T and SO64T glasses heat-treated at 900 °C for 2 h shows the effect of lithium content on crystallization. The scanning electron micrographs of the glass-ceramic samples show an increase in the crystal size with increase in the crystalline  $\beta$ -spodumene content (figures 4a to c). As seen in the micrograph of the sample SO46T with the highest K-content (figure 4a), the main crystalline phase is a high quartz and the crystalline particles are almost uniformly monosized and mainly of spherical shape ( $\approx 0.16$  to  $\approx 0.9 \mu\text{m}$ ) in glassy matrix. In the sample SO64T with the highest Li-content (figure 4c), the main crystalline phase is  $\beta$ -spodumene and the crystalline particles are nonuniform. The crystal growth rate was observed in the latter sample particularly in the irregular (maximum length was  $\approx 4 \mu\text{m}$ ) and the rod (maximum length was  $\approx 1.84 \mu\text{m}$ ) particles. Sample SO55T (figure 4b) had a microstructure midway between the crystallized SO46T and SO64T samples (compare figures 4a to c).

As observed from the microstructures, three different crystalline habitus are visible (figures 4a to c). As seen from the ratios of crystalline particles and the corresponding



Figures 4a to c. SEM micrographs of a) SO46T, b) SO55T, and c) SO64T glass samples heat-treated at 900 °C/2 h.

XRD patterns of the samples treated at 900 °C (figures 2a and 3a), if the spherical particles referred to high quartz, the main phase in the SO46T sample, then the rod and irregular ones may be assigned to leucite and  $\beta$ -spodumene, respectively.

Generally, the present microstructures were influenced by the  $\text{Li}_2\text{O}/\text{K}_2\text{O}$  ratios or the crystallization of high quartz and  $\beta$ -spodumene ratios. Increase in the  $\text{Li}_2\text{O}/\text{K}_2\text{O}$  ratio means an increase in the formation of  $\beta$ -spodumene accompanied by an increase in the crystal growth rate.

### 3.4 Thermal expansion characteristics

The effects of the glass composition on the glass transition ( $T_g$ ), glass softening ( $T_s$ ) and on the coefficient of thermal

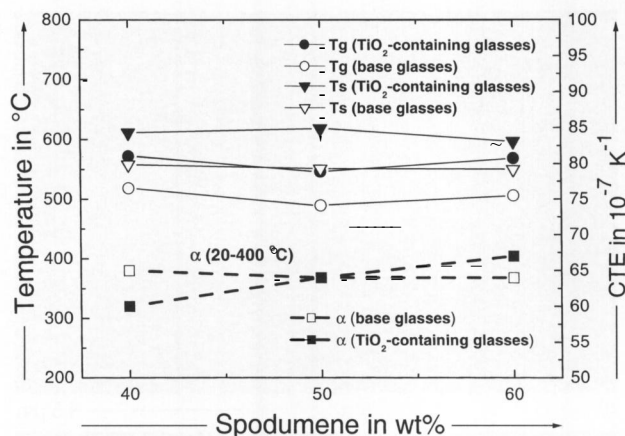


Figure 5. Change in CTE,  $T_g$  and  $T_s$  values as a function of the nominal spodumene ratio in base and  $\text{TiO}_2$  containing glasses.

Table 3. Transition temperature  $T_g$  and softening temperature  $T_s$  in  $^\circ\text{C}$ , and coefficient of thermal expansion  $\alpha$  in  $10^{-7} \text{K}^{-1}$  of the glass samples with and without  $\text{TiO}_2$

glass code	$T_g$	$T_s$	$\alpha_{20 \text{ to } 300^\circ\text{C}}$	$\alpha_{20 \text{ to } 400^\circ\text{C}}$	$\alpha_{20 \text{ to } 500^\circ\text{C}}$
SO46	518	572	66	65	65
SO46T <sup>*)</sup>	558	611	60	60	60
SO55	489	546	66	64	—
SO55T <sup>*)</sup>	551	618	68	68	69
SO64	506	569	66	64	—
SO64T <sup>*)</sup>	550	597	67	67	67

<sup>\*)</sup> With 3.0 wt%  $\text{TiO}_2$ .

expansion (CTE) are shown in figure 5 and table 3. It is observed that the glass transition temperature and the CTE are sensitive to the glass composition. However, there is little change in the values of  $T_g$  and  $T_s$  in both the base and the  $\text{TiO}_2$  containing glasses. In the base glasses,  $T_g$  and  $T_s$  ranged from 489 to 518  $^\circ\text{C}$  and from 546 to 572  $^\circ\text{C}$ , respectively. The incorporation of  $\text{TiO}_2$  increases these values from 550 to 558  $^\circ\text{C}$  for  $T_g$  and from 597 to 611  $^\circ\text{C}$  for  $T_s$  (table 3). The base glasses yield almost similar CTE in different temperature ranges with values ranging in between 64 to 66  $\cdot 10^{-7} \text{K}^{-1}$ . However, in  $\text{TiO}_2$  containing glasses, little variation in CTE value was detected which ranged in between 60 to 69  $\cdot 10^{-7} \text{K}^{-1}$  (table 3).

The experimental values of CTE of the SO46T and SO64T glasses heat-treated at 650  $^\circ\text{C}/5 \text{h}$  and 850  $^\circ\text{C}/5 \text{h}$ , given in table 4, decrease from 37 to 69  $\cdot 10^{-7} \text{K}^{-1}$ . The content of crystallized  $\beta$ -spodumene and the residual glass can depict the increase and decrease in CTE in the glass-ceramic samples. Based on such content and the accompanying residual glass, the CTE of the glass-ceramics decreases down to 37  $\cdot 10^{-7} \text{K}^{-1}$  at 20 to 300  $^\circ\text{C}$  in the SO64T sample and increases up to 69  $\cdot 10^{-7} \text{K}^{-1}$  at 20 to 300  $^\circ\text{C}$  in the SO46T sample.

In previous work, the CTE value of leucite containing glass-ceramic is quite high and ranges from 149 to 182.5  $\cdot 10^{-7} \text{K}^{-1}$  [11], whereas the CTE value of  $\beta$ -spodumene is very low with  $\approx 9 \cdot 10^{-7} \text{K}^{-1}$  [24]. In the present glass-ceramic samples the higher CTE values (68 to 69  $\cdot$

Table 4. Thermal expansion coefficient  $\alpha$  in  $10^{-7} \text{K}^{-1}$  of  $\text{TiO}_2$  containing glasses heat-treated at 650  $^\circ\text{C}/5 \text{h}$  + 850  $^\circ\text{C}/5 \text{h}$

glass code	$\alpha_{20 \text{ to } 300^\circ\text{C}}$	$\alpha_{20 \text{ to } 400^\circ\text{C}}$	$\alpha_{20 \text{ to } 500^\circ\text{C}}$	crystalline phase
SO46T <sup>*)</sup>	69	68	68	$\beta$ -spod(l) + leu(l)
SO64T <sup>*)</sup>	37	38	40	$\beta$ -spod + leu

<sup>\*)</sup> With 3.0 wt%  $\text{TiO}_2$ .

$10^{-7} \text{K}^{-1}$ ) were obtained in the sample of dominant high quartz and the lower values (37 to 40  $\cdot 10^{-7} \text{K}^{-1}$ ) resulted in the sample of dominant  $\beta$ -spodumene. However, the increase in CTE value was accompanied by an increase in the residual glass.

#### 4. Conclusion

In the binary spodumene-orthoclase glasses, within the  $\text{Li}_2\text{O}-\text{K}_2\text{O}-\text{Al}_2\text{O}_3-\text{SiO}_2$  system, the base glasses did not show any crystallization tendency, however, the incorporation of  $\text{TiO}_2$  encourages the crystallization behaviour. The developed crystalline phases were  $\beta$ -spodumene, leucite and high quartz. In the  $\text{K}_2\text{O}$ -rich glasses, the metastable high quartz was crystallized as the main phase, however, it decreases as little and minor phase with increasing the  $\text{Li}_2\text{O}$  in glass composition. Moreover, it disappeared at temperatures higher than 900  $^\circ\text{C}$ . The microstructure of crystallized glasses changes from fine uniform microstructure with domination of the high quartz to relatively nonuniform one with domination of the  $\beta$ -spodumene phase.

The values of CTE were between 60 and 69  $\cdot 10^{-7} \text{K}^{-1}$ , in both the base and the  $\text{TiO}_2$  containing glasses. The values of CTE of glass-ceramic samples were between 37 and 69  $\cdot 10^{-7} \text{K}^{-1}$ , however, the lower values indicate the domination of  $\beta$ -spodumene and the higher values refer to the increase in residual glass.

#### 5. References

- [1] Kingery, W. D.; Bowen, H. K.; Uhlmann, D. R.: Introduction to ceramics. New York: Wiley, 1976.
- [2] Höland, W.; Beall, G.: Glass-ceramic technology. Westerville, OH: The American Ceramic Society, 2002.
- [3] Höland, W.; Rheinberger, V.; Frank, M.: Mechanism of nucleation and controlled crystallization of needlelike apatite in glass-ceramics of the  $\text{SiO}_2-\text{Al}_2\text{O}_3-\text{K}_2\text{O}-\text{CaO}-\text{P}_2\text{O}_5$  system. *J. Non Cryst. Solids* **253** (1999) pp. 170–177.
- [4] Weinberg, M. C.: Transformation kinetics of particles with surface and bulk nucleation. *J. Non-Cryst. Solids* **142** (1992) pp. 126–232.
- [5] Schmelzer, J.; Pascova, J.; Moller, K. et al.: Surface-induced devitrification of glasses: the influence of elastic strains. *J. Non-Cryst. Solids* **162** (1993) pp. 26–39.
- [6] Höland, W.; Martin, F.; Rheinberger, V.: Surface crystallization of leucite in glasses. *J. Non-Cryst. Solids* **180** (1995) pp. 292–307.
- [7] Tosic, M. B.; Mitrovic, M. M.; Dimitrijevic, R. Z.: Crystallization of leucite as the main phase in aluminosilicate glass with low fluorine content. *J. Mater. Sci.* **35** (2000) pp. 3665–3667.
- [8] Mazza, D.; Lucco Borlera, M.; Brisi, C. et al.: Boron for aluminum substitution in the  $\text{KAlSi}_2\text{O}_6$  leucite structure. *J. Eur. Ceram. Soc.* **17** (1997) pp. 951–955.

- [9] Barlow, S. G.; Manning, D. A. C.: Influence of time and temperature on reactions and transformations of muscovite mica. *British Ceram. Trans.* **98** (1999) pp. 122–126.
- [10] Albakry, M.; Guazzato, M.; Swain, M.: Fracture toughness, microstructure and toughening mechanism of leucite and lithium disilicate glass ceramics. *Bioceram.* **15** (2003) pp. 955–958.
- [11] Ermich, M.; Kunzmann, K.; Assmann, S.: Röntgenographische Untersuchungen im System leucit-haltiger Dental-Keramiken. Poster at Meeting of Deutsche Gesellschaft für Kristallographie, Bayreuth 2001.
- [12] Strnad, Z.: *Glass-ceramic materials*. Amsterdam: Elsevier, 1986.
- [13] Priller, S.; Frischat, G. H.; Pye, L. D.: Strengthening of glass through surface crystallization of  $\beta$ -spodumene. *J. Non-Cryst. Solids* **196** (1996) pp. 144–149.
- [14] Kangguo, C.: Carbon effects on crystallization kinetics of  $\text{Li}_2\text{O}-\text{Al}_2\text{O}_3-\text{SiO}_2$  glasses. *J. Non-Cryst. Solids* **238** (1998) pp. 152–157.
- [15] El-Shennawi, A. W. A.; Hamzawy, E. M. A.; Khater, G. A. et al.: Crystallization of some aluminosilicate glasses. *Ceram. Int.* **27** (2001) pp. 725–730.
- [16] Powder Diffraction File Card No. 38-1423. The International Centre for Diffraction Data (ICDD), Newton Square, PA. (Formerly: Joint Committee for Powder Diffraction Standards (JCPDS).)
- [17] Powder Diffraction File Card No. 11-252. International Centre for Diffraction Data (ICDD), Newton Square, PA. (Formerly: Joint Committee for Powder Diffraction Standards (JCPDS).)
- [18] Doherty, P. E.; Lee, D. W.; Davis, R. S.: Direct observation of the crystallization of  $\text{Li}_2\text{O}-\text{Al}_2\text{O}_3-\text{SiO}_2$  glasses containing  $\text{TiO}_2$ . *J. Am. Ceram. Soc.* **50** (1967) pp. 77–81.
- [19] Beall, G. H.; Chyung, K.; Pierson, J. E.: Negative eucryptite glass-ceramics for fiber bragg grating athermalization. In: *Proc. XVIII International Congress on Glass*, San Francisco, CA, 1998. (Available on CD ROM.)
- [20] Ohlberg, S. M.; Golob, H. R.; Strickler, D. W.: Crystal nucleation by glass in glass separation. In: Reser, M. K.; Smith, G.; Insley, H. (eds.): *Symposium on Nucleation and Crystallization in Glasses and Melts*. Columbus, OH: The American Ceramic Society, 1962. Pp. 55–62.
- [21] Omar, A. A.; El-Shennawi A. W. A.; El-Ghannam, A. R.: Crystallization of some spodumene-lithium zinc orthosilicate glasses. *J. Mater. Sci.* **26** (1991) pp. 3366–3373.
- [22] Zarzycki, J.: *Glasses and the vitreous state*. Cambridge: Cambridge University Press, 1991. (Cambridge Solid State Science Series.)
- [23] Scholze, H.: *Glass: Nature, structure and properties*. New York et al.: Springer, 1991.
- [24] McMillan, M. W.: *Glass-ceramic*. 2<sup>nd</sup> ed. London: Academic Press, 1979.

■ E404P003

## Contact:

Ass. Prof. E. M. A. Hamzawy  
Glass Research Dept.  
National Research Centre  
Tahrir St. Dokki P.C. 12622  
Egypt  
E-mail: ehamzawy@lycos.com